**Osteogenic potential for replacing cells in rat cranial defects implanted with a DNA/protamine complex past**

Masako Toda[a], Jun Ohno[b*], Yosuke Shinozaki[c], Masao Ozaki[a], Tadao Fukushima[d]

[a]Department of Oral Growth and Development, Division of Pediatric Dentistry, Fukuoka Dental College, Fukuoka, Japan

[b]Department of Morphological Biology, Division of Pathology, Fukuoka Dental College, Fukuoka, Japan

[c]Department of Oral Rehabilitation, Section of Fixed Prosthodontics, Fukuoka Dental College, Fukuoka, Japan

Research Center for Regenerative Medicine, Fukuoka Dental College, Fukuoka, Japan

*Correspondence to: Jun Ohno DDS, PhD
Department of Morphological Biology, Division of Pathology,
Fukuoka Dental College, 2-15-1 Tamura, Fukuoka8140193, Japan
TEL: +81928010411
FAX: +81928014909
e-mail: johno@college.fdcnet.ac.jp

**Abstract**

Osteoinductive scaffolds are required for bone tissue engineering. The aim of the present study was to assess the osteoinductive capacity of deoxyribonucleic acid (DNA)/protamine complexes in a rat model of critical-size calvarial defects. In addition, we investigated whether cultured mesenchymal-like cells (DP-cells) outgrown from DNA/protamine complex engrafted defects could differentiate to become osteogenic cells *in vitro*. DNA/protamine complexes were prepared by reactions between DNA and protamine sulfate solutions with stirring. Critical-sized (8 mm) calvarial defects were created in the central parietal bones of adult rats. Defects were either left empty or treated with DNA/protamine complex scaffolds. Subsequently, micro-computed tomography (micro-CT), histological, and immunohistochemical analyses were performed. DP-cells were expanded from explants of DNA/protamine complex engrafted defects using an explant outgrowth culture system. Osteogenesis-related factors were assessed in DP-cells after treatment with an osteoblast-inducing reagent (OIR). After 3 months, nearly complete healing was observed for DNA/protamine complex engrafted calvarial defects. Increased alkaline phosphatase (ALP) activity and Alizarin red staining were found for cultured DP-cells. These cells had high expression levels of osteogenic genes, including those for RUNX-2, ALP, osteopontin, and osteocalcin. These results indicated that DNA/protamine complexes could facilitate bone regeneration in calvarial defects. Moreover, *in vitro* osteogenic induction experiments

showed that DP-cells outgrown from DNA/protamine engrafted defects had an osteogenic potential. Based on these results, we suggest that DNA/protamine complexes may recruit osteocompetent cells in these defects, where they differentiate to osteogenic cells.

Key words: DNA/protamine complex, scaffold, critical-size bone defect, bone regeneration, explant outgrowth culture

## Introduction

Satisfactory bone regeneration is necessary for healing critical-size bone defects (CSD) after skeletal injuries in orthopedic surgery, neurosurgery, and dentistry. Traditional treatments for CSD involve supplemental bone grafting, which depends on the most common sources of harvested tissue, including bone auto- and allografts. Among bones that are harvested, autogenous bone is regarded as the gold standard for bone graft materials because it provides the three elements necessary to generate and maintain the bone: scaffolding for osteoconduction; growth factors for osteoinduction; and progenitor cells for osteogenesis [1]. However, both auto- and allogenic bone harvests are limited in supply and associated with considerable donor site morbidities.

Recent strategies for bone tissue engineering have focused on creating tissue engineered constructs that include cells to be transplanted embedded within supporting matrices and biomolecules [2, 3]. This approach incorporates an interactive triad of viable osteocompetent cells, soluble osteoinductive signals, and osteoconductive matrices or scaffolds, with the aim of favorable bone regeneration within the defects [3, 4].

Optimal scaffolds are required for both tissue engineered constructs and for host tissues around these defects. For the engineered construct, the scaffolds must be able to deliver osteogenic cells and osteoinductive growth factors [5]. These scaffolds serve as a temporary matrix for cell migration, cell proliferation, and the deposition of extracellular

matrix components, with subsequent bone in-growth until a new bony tissue is totally regenerated [6]. In addition to biocompatibility, porosity, and surface properties, biodegradability and osteoinductivity are essential scaffold properties. Biodegradable scaffolds obviate the need for a second surgical procedure. These scaffolds should also be osteoinductive because they will stimulate osteocompetent cells that are recruited to a bone healing site and will undergo the osteogenic differentiation pathway [7].

We previously developed a biodegradable biomaterial comprising a mixture of salmon serum deoxyribonucleic acid (DNA) and protamine to be used as a scaffold for tissue engineering or drug delivery systems [8, 9]. The complex mixture prepared from DNA (mean of 300 base-pairs) and protamine could be turned into a paste by kneading in water [9, 10]. This paste had suitable viscosity for clinical use. These DNA/protamine complexes also had favorable properties for biomaterials, such as a high affinity for calcium ions [10] and antibacterial activity [11]. The complex powder also showed no adverse effects for MC3T3-E1 osteoblast-like cells, and had mild antibacterial activities and mild soft tissue responses [9].

In addition, our group previously implanted these DNA/protamine complexes in calvarial defects created in rats and demonstrated that these complexes induced bone regeneration [12]. These results led us to hypothesize that these DNA/protamine complexes could stimulate osteocompetent cells, recruit them to a bone healing site, and undergo

osteogenic differentiation during the healing process.

Thus, the aim of the present study was to assess the osteoinductive capacity of our DNA/protamine complexes in a rat model of CSD. In addition, we investigated whether cultured mesenchymal cells outgrown from DNA/protamine complex engrafted CSD could differentiate to become osteogenic cells *in vitro*.

## Materials and methods

### *Preparation of DNA/protamine complex paste disks*

DNA/protamine complex paste disks were prepared as previously described [12]. In brief, a solution of 300-bp fragments of sterilized salmon testis DNA was prepared and a 2% sterilized salmon testis protamine sulfate (MW = 4500) solution was provided by Maruha-Nichiro Holdings, Ltd., Tokyo, Japan. Freeze–dried DNA/protamine complex powder was kneaded in distilled water to convert it into a paste. To prepare disks of this DNA/protamine complex paste, the DNA/protamine complex paste was injected into a silicone mold (internal diameter: 8 mm; height: 0.8 mm) on a Teflon plate. The fabricated complex disks (40 mg) were immediately and carefully removed from the Teflon plate and silicone mold. All procedures were performed under sterile conditions using sterilized instruments and materials.

### *Rat model of critical-size calvarial bone defects*

Disk implantation was performed as previously described [12]. In brief, 10-week-old

male Sprague–Dawley (SD) rats (weight approximately 300 g) were anesthetized with 2% isoflurane (Abbott Laboratories, Abbott Park, IL, USA) and an air mixture gas flow of 1.0 L/min using an anesthesia gas machine (Anesthesia Machine SF-B01; MR Technology, Inc., Tsukuba, Ibaraki, Japan). A critical-size calvarial bone defect CSD was created and treated with an 8-mm diameter paste disk for different observation times (1, 2, and 3 months) [12, 13]. A control group included rats with CSD without these disks. Three rats were used for each group for each time period. Our animal experimentation protocols were approved by the Animal Care and Use Committee of Fukuoka Dental College (No. 10017).

***Bone regeneration evaluations***

Bone regeneration was evaluated using an *in vivo* micro-computed tomography (micro-CT) system (Skyscan-1176 micro-CT; Bruker, Kontich, Belgium) at 50 kVp and 500 μA for rats while under anesthesia (as described above) at 1, 2, and 3 months after disk implantation. Each image data set consisted of a scan size of approximately 35 μm. The percentage of the newly formed bone in a calvarial bone defect (New-Bone%) was calculated as previously described [12].

After micro-CT scanning, rats were sacrificed by injecting an overdose of isoflurane. Following which, the cranial tissues that contained untreated or treated samples were immediately excised. These samples were divided into three groups. For the first group of samples, tissue specimens were fixed in 4% paraformaldehyde in phosphate-buffered saline

(PBS), decalcified in 10% ethylenediamine tetraacetic acid (EDTA) for 4 weeks at 4°C, and then embedded in paraffin. Paraffin sections (4 μM) were then stained with hematoxylin and eosin (H&E) to visualize any histological changes.

The second group of samples was immediately frozen in liquid nitrogen. Non-decalcified frozen sections were processed for immunohistochemistry using primary rabbit anti-RUNX2 and mouse anti-osterix antibodies (1:100; Abcam) and goat anti-rabbit or mouse immunoglobulin G (IgG) conjugated with Alexa Fluor 488 or 568 (1:200; Molecular Probes, Eugene, OR, USA). To visualize nuclei, immunostained cells were counterstained with 4,6-diamidino-2-phenylindole (DAPI; Vector Laboratories Inc., Burlingame, CA, USA).

The third group of samples (used as non-decalcified specimens) was stained with Villanueva osteochrome bone (VOB) stain. For VOB staining, specimens were immersed in VOB solution for 3 days, dehydrated with a graded ethanol series, defatted in acetone, and then embedded in methyl methacrylate. These specimens were sectioned at 20 μm. The stained sections were observed for histology by fluorescence microscopy.

***Explant outgrowth culture of fibrous connective tissue from calvarial defects***

Fibrous connective tissue (Fig. 1a) from the CSD at 2 weeks after DNA/protamine complex paste disk implantation and normal periosteum tissue (Fig. 1b) were used for an explant outgrowth culture system. Primary cultures of mesenchymal cells (DP-cells) and periosteal cells (PO-cells) were obtained as outgrowths from the explants of connective tissue

from the CSD and periosteum tissue, respectively. The tissues were cut into pieces of approximately 3 × 2 × 2 mm and placed on the bottoms of dishes. They were allowed to adhere to these dishes and then cultured in Dulbecco's modified Eagle's medium (DMEM; Invitrogen, Tokyo, Japan) supplemented with 10% (v/v) fetal bovine serum (FBS; HyClone, Logan, UT, USA) and 1% (v/v) penicillin/streptomycin (PS; Invitrogen). All cultures were maintained at 37°C in a humidified incubator and with 5% $CO_2$. After 21 days, outgrown cells from the explants were subcultured and maintained for up to an additional 7 days as secondary monolayers on tissue culture dishes before being used for assays.

***ALP assays***

The effect of an osteoblast-inducer reagent (OIR) on alkaline phosphatase (ALP) in DP- and PO-cells was assessed by determining ALP activity and staining. Both cell types were seeded at a density of $10^5$ cells/well in 24-well microplates and exposed to DMEM with 10% (v/v) and 1% (v/v) PS before incubation for 7 days at 37°C in an atmosphere of 5% $CO_2$. To induce the differentiation of both cell types, the medium was replaced every 2 days with DMEM with 10% (v/v) FBS that was supplemented with OIR (Takara Bio Inc., Otsu, Japan), which included ascorbic acid, hydrocortisone, and β-glycerophosphate. The cells were cultured for 3, 7, 14, and 21 days.

After incubation for the indicated time, the ALP activity was determined using a phosphatase substrate kit (AnaSpec, Inc., Fremont, CA), according to the manufacturer's

instructions. Optical densities were measured using a microplate reader at 405 nm. The results were obtained for triplicate samples and given as means ±standard deviations (SD's). ALP expression was assessed in differentiated cells induced by OIR using an ALP staining kit (Takara Bio Inc., Otsu, Japan), according to the manufacturer's instructions.

***Alizarin red staining***

Both DP- and PO-cells were seeded at a density of $10^5$ cells/well in 24-well microplates and exposed to DMEM with 10% (v/v) FBS and 1% (v/v) PS before incubation for 7 days at 37°C in an atmosphere of 5% $CO_2$. Osteogenic differentiation was induced by replacing the medium every 2 days with DMEM with 10% (v/v) FBS and OIR. After differentiation for 14 days, the cells were washed twice with PBS, fixed for 10 min in 4% paraformaldehyde in PBS, and then rinsed twice with distilled water. These cells were stained at room temperature for 5 min with Alizarin red, excess dye was removed, and the cells were washed with distilled water. Any calcified deposits that had stained red were photographed.

***Real-time reverse transcription-polymerase chain reaction (qRT-PCR)***

Total ribonucleic acid (RNA) was isolated from tissues of DNA/protamine complex paste disk-implanted defects and normal periosteum, and DP- and PO-cells treated with OIR using an ISOGEN Kit (Roche Diagnostics, Tokyo, Japan), according to the manufacturer's instructions. Total RNA (1 μg) was transcribed into cDNA using random and Oligo (dT) primers and reverse transcriptase in a total volume of 10 μl (ReverTra® Ace qPCR RT Kit;

Toyobo Co., Ltd., Osaka, Japan). Reverse transcription was performed at 37°C for 15 min and then at 98°C for 5 min. The resulting templates were subjected to a LightCyclerNano real-time polymerase chain reaction (PCR) system according to the manufacturer's protocol (Roche Diagnostics, Tokyo, Japan). Glyceraldehyde-3-phosphate dehydrogenase (G3PDH) was used as an internal control. Relative mRNA expression was determined as the ratio of RUNX-2, ALP, osteopontin (OPN), or osteocalcin (OCN) gene mRNA to G3PDH mRNA. All reactions were run in triplicate. The primers used and TaqMan probes were as follows: G3PDH forward primer 5′-AATGTATCCGTTGTGGATCTGA-3′ and reverse primer 5′-GCTTCACCACCTTCTTGATGT-3′, Universal ProbeLibrary probe no. 80; RUNX-2 forward primer 5′ -GGCCCTGGTGTTTAAATGG-3′ and reverse primer, 5′ -AGCACTCACTGACTCGGTTG-3′, Universal ProbeLibrary probe no. 83; ALP forward primer 5′-ACGAGGTCACGTCCATCCT-3′ and reverse primer, 5′-CCGAGTGGTGGTCACGAT-3′, Universal ProbeLibrary probe no. 89; OPN forward primer 5′-GGCTACAGCATCTGAGTGTTTG-3′ and reverse primer, 5′-CGGTGAAAGTGGCTGAGTTT-3′, Universal ProbeLibrary probe no. 82; OCN forward primer 5′-ATAGACTCCGGCGCTACCTC-3′ and reverse primer, 5′-GCTTCACCACCTTCTTGATGT-3′, Universal ProbeLibrary probe no. 125.

***Immunocytochemistry***

DP- and PO-cells were seeded on 13-mm cover glasses and cultured for 3, 7, 14, and

21 days. After culture for the indicated time, cells were fixed with 4 % paraformaldehyde for 10 min and washed in 0.1% Triton X-100 in PBS for 15 min. We simultaneously performed two types of double immunofluorescence staining for both cell types using two mixtures of two primary antibodies: (1) mouse monoclonal anti-rat prolyl-4-hydroxylase β (PHB, 1:100; Acris Antibodies GmbH, Herford, Germany) and rabbit polyclonal anti-RUNX-2 (1:100; Abcam, Tokyo, Japan); and (2) monoclonal anti-rat PHB (1:100; Acris Antibodies) and rabbit polyclonal anti-rat Sp7/osterix (1:100; Abcam), at 4°C overnight. After washing with PBS, cells were incubated in a mixture of anti-mouse IgG antibody conjugated with Alexa Fluor 488 (1:200; Molecular Probes, Eugene, OR, USA) and anti-rabbit IgG antibody (1:200; Molecular Probe) at room temperature for 30 min.

***Statistical analysis***

The results are given as means ±SD's. The group results were compared by one-way analysis of variance (ANOVA) and Scheffe's multiple comparisons tests. A $p$ value of $<0.05$ was considered significant.

**Results**

***DNA/protamine complexes heal critical-size rat calvarial defects***

To evaluate the potential for bone regeneration by our DNA/protamine complexes, CSD were created in the calvarial bones of 10-week-old SD rats. These CSD cannot spontaneously heal during the bone healing period [14]. We first used micro-CT scanning and low-magnification

images of H&E stained sections to assess bone regeneration. By 2 months postoperatively, micro-CT analyses showed that these defects had no evidence of new bone formation in the untreated rats, in agreement with the histological evidence (Fig. 2, upper and middle images at left). In the DNA/protamine complex-implanted defects, micro-CT scans showed small peninsulas at 1 month. Histologically, H&E-stained sections showed no residual materials within any of the defect regions and extensions of new bones from the edges of these defects (Fig. 2, upper images at right). Both micro-CT and histological analyses showed an increase in peninsula extension at 2 months in the defects that had been implanted with DNA/protamine complexes (Fig. 2, middle images at right). In the untreated defects at 3 months, small peninsulas were observed by both micro-CT and histological analyses (Fig. 2, lower images at left). However, at 3 months, enhanced bony regeneration was observed in the defects that had been implanted with DNA/protamine complexes by both micro-CT and histological examinations (Fig.2, lower images at right).

We next quantified these micro-CT images for the percentage of defect healing by quantifying the pixels in these defects. Percentage healing was determined by dividing the defect area by the defect size immediately postoperatively. These results are summarized in Figure 3. Compared with the untreated rats (white bars), DNA/protamine complex-implanted rats (black bars) consistently showed higher percentages of new bone areas at each time point. In the untreated rats, the empty defects had healed by less than 20% over the course of

3 months. In contrast, the defects that were treated with DNA/protamine complexes showed >70% healing after 3 months. These results demonstrated that these DNA/protamine complexes could promote bone regeneration in rat calvarial CSD.

***Histological bone healing processes in calvarial defects***

We next investigated how these micro-CT findings reflected the histological bone healing processes in calvarial CSD at each time point using higher magnifications for the H&E-stained sections. By 1 month after implantation, the defects had been replaced by a dense fibrous connective tissue that contained no material residues and a newly formed bone had extended from the edges of these defects (Fig. 4a). Red immunofluorescence after VOB staining was observed in new bone extensions, which indicating that this newly formed bone was immature (Fig. 4d).

Associated with the continuous extensions of a new bone from the edges of these defects, bone formation islands were observed in the fibrous connective tissue at 2 months after implantation (Fig. 4b). VOB staining showed that both extension areas and new bone islands consisted of immature bone (Fig. 4e). Greater bone formation was observed at 3 months after implanting DNA/protamine complexes (Fig. 4c). By VOB staining, most of the bone that had been replaced was in a mature condition, other than the peripheral areas of the bone (Fig. 4f). These histological changes corresponded well with the micro-CT data.

***Tissue expression of osteogenic markers in calvarial defects implanted with***

***DNA/protamine***

To determine if the cells included in the defects implanted with DNA/protamine complexes had osteoblastic properties, we immunostained non-decalcified frozen sections of these calvaria at 1 month after DNA/protamine complex implantation using an anti-RUNX-2 antibody, a known osteoblast marker. RUNX-2 nuclear expression was observed in spindle-shaped cells of fibrous connective tissue in these defects (Fig. 5a).

We also examined the tissue expression of osteogenic genes' mRNA by qRT-PCR. This indicated that the relative ALP and OCN mRNA expression levels (normalized to G3PDH mRNA expression) were increased by 33.3-fold and 5.4-fold, respectively, compared with that in normal periosteum (Fig. 5b). Relative RUNX-2 and OPN mRNA expression was slightly increased as compared with that in normal periosteum. These results indicated that the replacement tissue in those defects implanted with DNA/protamine complexes contained numerous cells with osteoblastic potential.

***Morphological characteristics of DP-cells after explant outgrowth culture***

To determine the bone formation capacity of the cells that were replacing the calvarial defects, we developed an explant outgrowth culture system. DP-cells were cultured as explants of the fibrous connective tissue in the defects that had been implanted with DNA/protamine complexes using DMEM supplemented with 10% FBS. Cell growth by DP-cells was similar to that of PO-cells. Cell migration and growth from the explants of the

fibrous connective tissue in defects occurred within 6–7 days, which was later than that observed for periosteal cultures (4–5 days), as shown in Figures 6a and b. Healthy, confluent cultures of DP-cells were obtained within 3 weeks as compared with 10–14 days for periosteal culture. Although both cell types had spindle and/or polygonal shapes, cultured DP-cells (Fig. 6c) appeared to be slightly larger in size as compared with the cultured PO-cells (Fig. 6d).

***Increased ALP activity and induction of calcified deposits in DP-cells treated with OIR***

ALP activity is a well defined marker of osteogenesis and is assumed to reflect the degree of cell differentiation to osteoblasts [15]. We determined the ALP activity of DP- and PO-cells with and without OIR treatment for up to 21 days. We first examined the ALP activity in DP- and PO-cells cultured without OIR. At 14 days, there were no significant differences in the ALP activity or ALP staining intensity between both cell types cultured without OIR (Fig. 7). Figures 8a and b summarize the temporal changes in the ALP activity and ALP staining intensity for DP- and PO-cells cultured with OIR.

On day 3, there was no significant difference in the ALP activity between DP- and PO-cells. The ALP activity and staining intensity of DP-cells increased from day 7 and peaked on day 14. The ALP activity of these cells tended to decrease by day 21. Compared with PO-cells, the ALP activity of DP-cells increased on days 7 and 14 by approximately 1.4-fold and 11.2-fold, respectively, and was even approximately 8.1-fold higher on day 21.

These results indicated that DP-cells could differentiate to a progenitor condition for bone formation after OIR stimulation.

Alizarin red staining of cells was used to demonstrate a mineralized extracellular matrix as calcified deposits. We examined if DP-cells cultured with OIR exhibited a late period of matrix maturation. Almost all areas of the wells used for culture of DP-cells treated with OIR appeared red, whereas only tiny weak spots of Alizarin red staining were observed in wells used for culture of PO-cells (Fig. 8c). These results indicated that the DP-cells treated with OIR had more calcification than the corresponding PO-cells.

***Increased osteogenic genes' expression in DP-cells treated with OIR***

To further investigate whether osteogenic genes could be induced in DP-cells treated with OIR, relative RUNX-2, ALP, OPN, and OCN mRNA expressions were analyzed by qRT-PCR. We first examined osteogenic genes' mRNA expression in DP-cells cultured without OIR for 14 days. Compared with normal PO-cells, the relative OPN and OCN mRNA expression levels (normalized to G3PDH mRNA) were increased by 42.0-fold and 10.4-fold, respectively (Fig. 9). RUNX-2 and ALP mRNA expression was only slightly increased.

We also examined the temporal changes in the transcription levels of these marker genes in DP- and PO-cells treated with OIR, and compared these levels to those in PO-cells at day 0. These results are summarized in Figure 10. Relative RUNX-2 and OCN mRNA expression in DP-cells treated with OIR gradually increased after day 7 and peaked on day

21. On day 21, the RUNX-2 and OCN mRNA levels were upregulated by 3.3-fold and 16.2-fold, respectively, as compared with the levels in PO-cells. Relative ALP mRNA expression peaked on day 7 (4.2-fold higher). Relative OPN mRNA expression exhibited two peaks on days 0 (9.1-fold increase) and 14 (1.6-fold increase). These results indicated that DP-cells had osteogenic properties regardless of the culture conditions used.

***RUNX-2 protein expression in DP-cells treated with OIR***

We next examined protein expression for one of the osteogenic markers, RUNX-2, in DP- and PO-cells treated with OIR for 21 days by double immunocytochemistry analysis. Anti- proxyl-4-hydroxylase β was used as a marker of mesenchymal lineage for both cell types. These results showed that RUNX-2 was expressed in the nuclei of DP-cells (Fig. 11a). In contrast, only faint or negative staining was found for PO-cells (Fig. 11b).

**Discussion**

It is believed that efficient regeneration of bone defects can be achieved by a combination of three regenerative elements: scaffolds, cells, and growth factors. A number of scaffolds have been devised, including bioceramics, natural, and synthetic polymers, and applied clinically [16]. In the present study, we provided three lines of evidence that DNA/protamine complexes were osteoinductive factors for bone healing in rat calvarial CSD [12]. First, micro-CT and histological results confirmed that DNA/protamine complex engrafted defects had enhanced bone regeneration in our rat CSD model. Second, increased ALP activity and

induced calcified depositions were observed in OIR-cultured DP-cells that were outgrown from DNA/protamine complex engrafted defects. Third, qRT-PCR and immunocytochemical data indicated that OIR-cultured DP-cells exhibited the characteristics of osteogenic cells.

Micro-CT analysis of DNA/protamine complex engrafted CSD indicated that these complexes could induce efficient bone regeneration. Histological findings complemented these micro-CT results, in that they showed that the bone healing process consisted of new bone extensions from defect edges and islands of bone formation in connective tissue. The new bone extension from bone defect edges is believed to be typical of bone healing, as shown by alveolar bones in a socket when a tooth is extracted. The fibrous connective tissue of DNA/protamine complex engrafted defects contained a few islands of bones at 2 months after implantation.

The appearance of discontinuous bones likely explains why these DNA/protamine complexes have the potential for ectopic bone formation. These findings are supported by those in a previous report [12]. Moreover, immunohistochemical findings showed that the mesenchymal-like cells in defects expressed RUNX-2, indicating that there were numerous osteocompetent cells in DNA/protamine complex engrafted defects. Thus, these results provide additional support for the osteogenic potential of DNA/protamine complexes *in vivo*.

Our results suggested that mesenchymal-like cells accumulated in DNA/protamine complex engrafted defects and appeared to have osteogenic potential. Thus, we developed an

explant outgrowth culture system to examine if these cells, DP-cells, in engrafted defects had osteogenic properties after treatment with OIR. After expansion, these DP-cells were morphologically identical to PO-cells. However, their response to OIR was completely different from that of PO-cells.

The ALP activity of DP-cells peaked at 14 days after culture with OIR, which indicated that these cells had initiated osteoblastic differentiation because ALP levels are indicative of osteoblastic activity [15] and bone ALP is produced in extremely high amounts during the bone formation cycle [15]. After the peak in ALP activity, DP-cells exhibited a late period of osteoblastic differentiation, as shown by Alizarin red positive staining at 21 days. Because Alizarin red staining reflects a mineralized extracellular matrix produced by cells as calcified deposits, the maturation of DP-cells cultured with OIR proceeded with an increased ALP activity for 21 days. These *in vitro* results likely support the bone regeneration process in DNA/protamine engrafted defects.

Our qRT-PCR and immunocytochemical results complemented the osteoblastic differentiation of DP-cells cultured with OIR. We found that RUNX-2, ALP, OPN, and OCN gene expression was upregulated in DP-cells treated with OIR as compared with PO-cells. ALP and OPN mRNA expression levels were increased in DP-cells at days 7 and 14, respectively. After these peaks of increased expression, both expressions were dramatically decreased. The expression pattern of ALP mRNA was similar to that of the ALP activity,

even though increased ALP mRNA expression was earlier than that of the enhanced ALP activity.

OPN is a non-collagenous, secreted glycosylation phosphoprotein that is expressed during the early stage of osteogenesis and is mass-produced when calcification begins [17]. The peak in OPN mRNA expression on day 14 appeared to reflect the initiation of calcification in DP-cells after treatment with OIR. In contrast, increased RUNX-2 and OCN mRNA expression began and peaked at days 7 and 14, respectively.

RUNX-2 is one of the transcription factors for BMP2 target genes and is essential for the development of the osteoblast phenotype. It is known that RUNX-2 is required for osteoblast differentiation and bone formation at the later stages of embryonic development [18, 19]. OCN is a specific non-collagen protein that is secreted by osteoblasts and is used as a marker for the late stage of osteoblast differentiation [15, 19]. Therefore, both these genes may participate in the late stage of osteoblast differentiation. Our immunocytochemical analysis results complemented our qRT-PCR results by showing that RUNX-2 protein expression in DP-cells treated with OIR occurred at day 21 [20]. The higher expression levels of osteogenic genes and proteins by DP-cells cultured with OIR indicated that DP-cells had an enhanced capability to support osteogenic differentiation and/or maturation as compared with PO-cells.

In summary, we demonstrated that DNA/protamine complexes could facilitate bone

regeneration in rat calvarial defects. Our *in vitro* experiments for osteogenic induction showed that DP-cells outgrown from DNA/protamine engrafted defects had an osteogenic potential. Based on these results, we suggest that DNA/protamine complexes may recruit osteocompetent cells in these defects and differentiate to become osteogenic cells. However, the detailed mechanisms for enhanced bone regeneration by DNA/protamine remain unclear. Future studies will address the detailed effects of DNA/protamine on microenvironments to induce osteogenesis in these bone defects.

**Competing interests**

The authors declare that they have no competing interests.

**Acknowledgments**

The present study was supported in part by a Grant-in-aid for Scientific Research (B) (23390455) and by a Grant-in-aid for strategic study base formation support business (S1001059) from the Japan Society for the Promotion of Science. We thank Maruha-Nichiro Holdings for providing DNA and protamine. The authors would like to thank Enago (www.enago.jp) for the English language review.

**References**

1. Dimitriou R, Jones E, McGonagle D, Giannoudis PV. Bone regeneration: current concepts and future directions. BMC Med 2011; 9:66.

2. Hutmacher DW, Garcia AJ. Scaffold-based bone engineering by using genetically modified cells. Gene 2005; 347:1-10.

3. Sittinger M, Hutmacher DW, Risbud MV. Current strategies for cell delivery in cartilage and bone regeneration. Curr Opin Biotechnol 2004; 15:411-18.

4. Ramoshebi LN, Matsaba TN, Teare J, Renton L, Patton J, Ripamonti U. Tissue engineering: TGF-beta superfamily members and delivery systems in bone regeneration. Expert Rev Mol Med 2002; 4:1-11.

5. Seeherman H. The influence of delivery vehicles and their properties on the repair of segmental defects and fractures with osteogenic factors. J Bone Joint Surg Am 2001; 83: 79-81.

6. Hutmacher DW. Scaffolds in tissue engineering bone and cartilage. Biomaterials 2000; 21:2529-43.

7. Salgado AJ, Coutinho OP, Reis RL. Bone tissue engineering: state of the art and future trends. Macromol Biosci 2004; 4:743-65.

8. Fukushima T, Ohno J, Hayakawa T, Imayoshi R, Kawaguchi M, Doi Y, Kanaya K, Mitarai M. Polycationic protamine for water-insoluble complex formation with DNA. Dent Mater J 2010l; 29:529-35.

9. Fukushima T, Ohno J, Imayoshi R, Mori N, Sakagami R, Mitarai M, Hayakawa T. DNA/protamine complex paste for an injectable dental material. J Mater Sci Mater Med

2011; 22: 2607-15.

10. Fukushima T, Ohno J, Hayakawa T, Kawaguchi M, Inoue Y, Takeda S, Toyoda M, Okahata Y. Mold fabrication and biological assessment of porous DNA-chitosan complexes. J Biomed Mater Res B Appl Biomater 2009; 91:746-54.

11. Johansen C, Gill T, Gram L. Antibacterial effect of protamine assayed by impedimetry. J Appl Bacteriol 1995; 78:297-303.

12. Shinozaki M, Yanagi T, Yamaguchi Y, Kido H, Fukushima T. Osteogenic evaluation of DNA/protamine complex paste in rat cranial defects. J Hard Tissue Biol 2013; 22:401-408.

13. Terella A, Mariner P, Brown N, Anseth K, Streubel SO. Repair of a calvarial defect with biofactor and stem cell-embedded polyethylene glycol scaffold. Arch Facial Plast Surg 2010; 12:166-71.

14. McKee MD, Nanci A. Osteopontin at mineralized tissue interfaces in bone, teeth, and osseointegrated implants: ultrastructural distribution and implications for mineralized tissue formation, turnover, and repair. Microsc Res Tech 1996; 33:141-64.

15. Christenson RH. Biochemical markers of bone metabolism: an overview. Clin Biochem 1997; 30:573-93.

16. Bessa PC, Casal M, Reis RL. Bone morphogenetic proteins in tissue engineering: the road from laboratory to clinic, part II (BMP delivery). J Tiss Engin Reg Med 2008; 2:81-96.

17. Schmitz JP, Hollinger JO. The critical size defect as an experimental model for

craniomandibulofacial nonunions. Clin Orthop Relat Res 1986; 205:299-308.

18. Hassan MQ, Tare RS, Lee SH, Mandeville M, Morasso MI, Javed A, van Wijnen AJ, Stein JL, Stein GS, Lian JB. BMP2 commitment to the osteogenic lineage involves activation of Runx2 by DLX3 and a homeodomain transcriptional network. J Biol Chem 2006; 281:40515-26.

19. Yang F, Yuan PW, Hao YQ, Lu ZM. Emodin enhances osteogenesis and inhibits adipogenesis. BMC Complement Altern Med 2014;14:74.

20. Zaidi SK, Young DW, Pockwinse SM, Javed A, Lian JB, Stein JL, van Wijnen AJ, Stein GS. Mitotic partitioning and selective reorganization of tissue-specific transcription factors in progeny cells. Proc Natl Acad Sci U S A 2003; 100:14852-57.

1. Hutmacher DW, Garcia AJ. Scaffold-based bone engineering by using genetically modified cells. Gene 2005;347:1-10.

2. Sittinger M, Hutmacher DW, Risbud MV. Current strategies for cell delivery in cartilage and bone regeneration. Curr Opin Biotechnol 2004;15:411-18.

3. Ramoshebi LN, Matsaba TN, Teare J, Renton L, Patton J, Ripamonti U. Tissue engineering: TGF-beta superfamily members and delivery systems in bone regeneration. Expert Rev Mol Med 2002;4:1-11.

4. Seeherman H. The influence of delivery vehicles and their properties on the repair of

segmental defects and fractures with osteogenic factors. J Bone Joint Surg Am 2001;83:79-81.

5. Hutmacher DW. Scaffolds in tissue engineering bone and cartilage. Biomaterials 2000;21:2529-43.

6. Salgado AJ, Coutinho OP, Reis RL. Bone tissue engineering: state of the art and future trends. Macromol Biosci 2004;4:743-65.

7. Fukushima T, Ohno J, Imayoshi R, Mori N, Sakagami R, Mitarai M, Hayakawa T. DNA/protamine complex paste for an injectable dental material. J Mater Sci Mater Med 2011;22:2607-15.

8. Fukushima T, Ohno J, Hayakawa T, Imayoshi R, Kawaguchi M, Doi Y, Kanaya K, Mitarai M. Polycationic protamine for water-insoluble complex formation with DNA. Dent Mater J 2010, 29:529-35.

9. Fukushima T, Ohno J, Hayakawa T, Kawaguchi M, Inoue Y, Takeda S, Toyoda M, Okahata Y. Mold fabrication and biological assessment of porous DNA-chitosan complexes. J Biomed Mater Res B Appl Biomater 2009, 91:746-54.

10. Johansen C, Gill T, Gram L. Antibacterial effect of protamine assayed by impedimetry. J Appl Bacteriol 1995;78:297-03.

11. Shinozaki M, Yanagi T, Yamaguchi Y, Kido H, Fukushima T. Osteogenic evaluation of DNA/protamine complex paste in rat cranial defects. J Hard Tissue Biol 2013;22:401-08.

12. Christenson RH. Biochemical markers of bone metabolism: an overview. Clin Biochem 1997;30:573-93.

13. Bessa PC, Casal M, Reis RL. Bone morphogenetic proteins in tissue engineering: the road from laboratory to clinic, part II (BMP delivery). J Tiss Engin Reg Med 2008;2:81-96.

14. Schmitz JP, Hollinger JO. The critical size defect as an experimental model for craniomandibulofacial nonunions. Clin Orthop Relat Res 1986;299-308.

15. Hassan MQ, Tare RS, Lee SH, Mandeville M, Morasso MI, Javed A, van Wijnen AJ, Stein JL, Stein GS, Lian JB. BMP2 commitment to the osteogenic lineage involves activation of Runx2 by DLX3 and a homeodomain transcriptional network. J Biol Chem 2006;281:40515-26.

16. Terella A, Mariner P, Brown N, Anseth K, Streubel SO. Repair of a calvarial defect with biofactor and stem cell-embedded polyethylene glycol scaffold. Arch Facial Plast Surg 2010;12:166-71.

17. Zaidi S K, Young D W, Pockwinse S M, Javed A, Lian J B, Stein J L, van Wijnen A J, Stein G S. Mitotic partitioning and selective reorganization of tissue-specific transcription factors in progeny cells. Proc Natl Acad Sci U S A 2003;100:14852–57.

18. Yang F, Yuan PW, Hao YQ, Lu ZM. Emodin enhances osteogenesis and inhibits adipogenesis. BMC Complement Altern Med 2014;14:74.

**Figure legends**

**Figure 1** Tissue explants for outgrowth culture. (a) Fibrous connective tissue (rectangle) was replaced in a DNA/protamine paste-implanted calvarial defect. (b) Periosteum (rectangle) in rat calvarial bone. The upper position of each picture is the skin side.

**Figure 2** Calvarial healing assessed by micro-computed tomography (micro-CT). Procedures for calvarial defects included no treatment (empty defects) and defects implanted with DNA/protamine complex paste disks. Micro-CT analysis and panoramic images of H&E staining up to 3 months (1 M, 2 M, and 3 M) revealed slight healing in empty defects. In contrast, DNA/protamine complexes nearly healed bone defects by 3 months.

**Figure 3** Quantitative results for micro-CT analysis. Healing of defects is shown as the fraction of new bone with respect to the total defect area as quantified by micro-CT analysis (N = 5/group) $*P < 0.05$, compared with untreated defects.

**Figure 4** Representative H&E and VOB staining images during bone regeneration in rat calvarial defects. (a)-(c) H&E staining of decalcified sections of defects after implanting DNA/protamine complexes at 1 (a), 2 (b), and 3 (c) months. (d)-(f) VOB staining for sections at 1 (d), 2 (e), and 3 (f) months. Bars = 500 μm.

**Figure 5 Tissue expression of osteogenic markers in calvarial defects implanted with DNA/protamine complexes.** (a) Non-decalcified frozen sections at 1 month were stained with anti-RUNX-2. (b) qRT-PCR analyses for RUNX-2, ALP, OPN, and OCN mRNA

expression (normalized to G3PDH mRNA) as compared with normal periosteum. Results are means ±SD's for 3-5 independent experiments.

**Figure 6 Growth initiation and morphological characteristics of connective tissue in bone defects and periosteal cultures.** Growth initiation from the explants of (a) connective tissue in defects (DP-cells) and (b) normal periosteum (PO-cells). Confluent cultures of (c) DP-cells and (d) PO-cells. *, indicates explants.

**Figure 7 ALP activities and staining intensities of DP- and PO-cells cultured without OIR** (a) ALP activity of DP- and PO- cells cultured without OIR for 14 days. (b) ALP staining for DP- and PO- cells cultured without OIR for 14 days.

**Figure 8 ALP activity and mineralization of DP-cells treated with OIR.** (a) Total ALP activity of DP- and PO- cells treated with OIR for a period of 21 days. ALP activity levels were compared between DP- and PO-cells treated with OIR. Results are means ±SD's for 5 independent experiments. *, significantly different at $P < 0.05$ compared with PO-cells. (b) ALP staining of DP- and PO-cells treated with OIR for a period of 21 days. Purple precipitates indicate ALP activity. (c) Cells from explants of DNA/protamine implanted tissue (DP-cells) or normal periosteal tissue (PO-cells) were incubated for 21 days without OIR (left) or with OIR (right). Matrix mineralization was visualized in OIR-cultured DP-cells by Alizarin red staining.

**Figure 9 Gene expression for osteogenesis markers in DP- and PO-cells without OIR**

**treatment for 14days.** qRT-PCR was used to determine RUNX-2, ALP, OPN, and OCN mRNA expression (normalized to G3PDH mRNA), as compared with normal periosteum. Results are means ±SD's for 3–5 independent experiments.

**Figure 10 Gene expression for osteogenesis markers in DP- and PO-cells treated with OIR.** qRT-PCR results for RUNX-2, ALP, OPN, and OCN mRNA expression in DP- cells (solid lines) and PO-cells (broken lines) treated with OIR. Results are mRNA fold-increases (normalized to GAPDH mRNA) and compared with results for PO-cells treated with OIR on day 0. Vertical lines represent means ±SD's of 3 independent experiments, each performed in triplicate. *, significantly different at $P < 0.05$ compared with PO-cells.

**Figure 11 Immunocytochemical analysis of RUNX-2 protein expression in DP-cells treated with OIR for 21days.** Double immunofluorescence images using antibodies specific for proxyl-4-hydroxylase β (green) and RUNX-2 (red) for (a) DP-cells and (b) PO-cells.

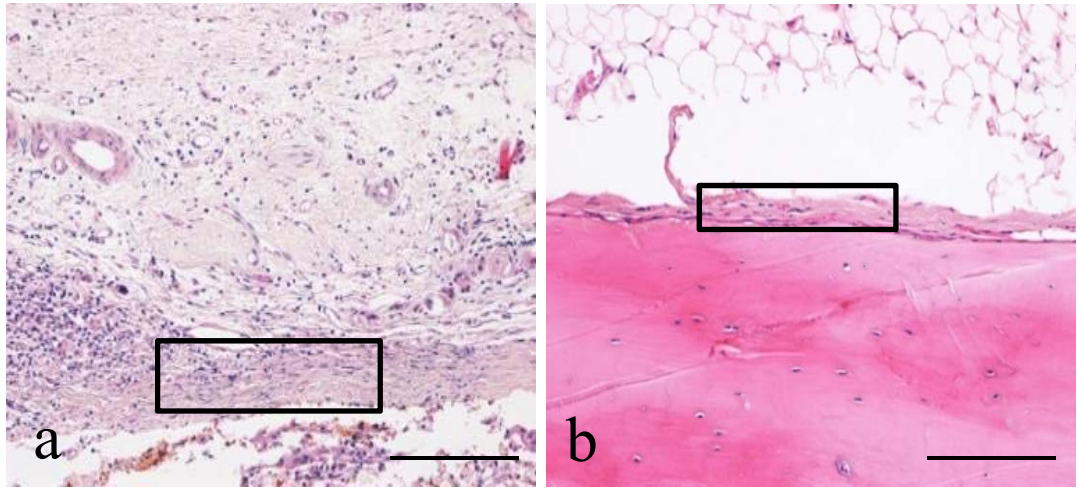


Fig. 1

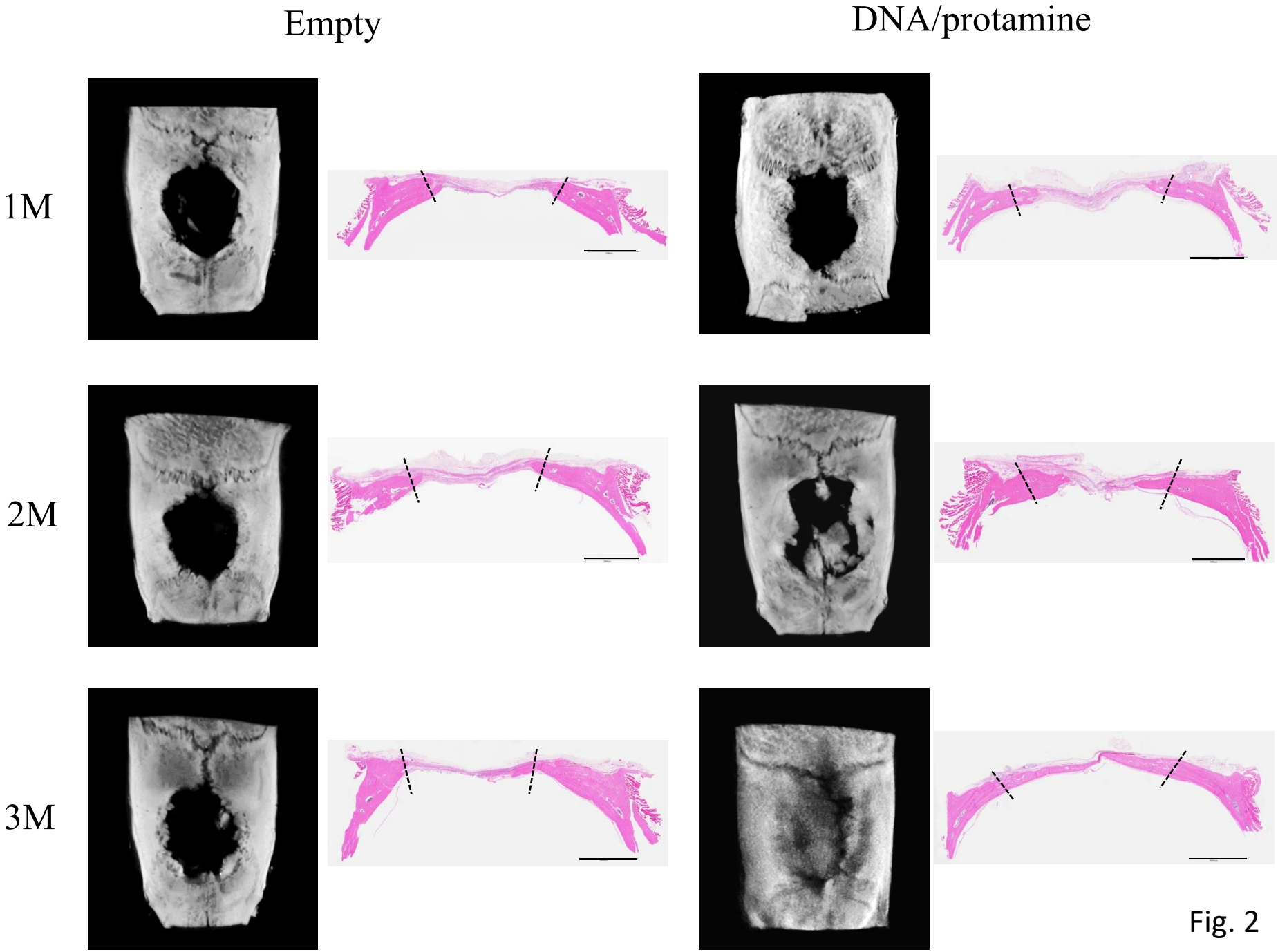


Fig. 2

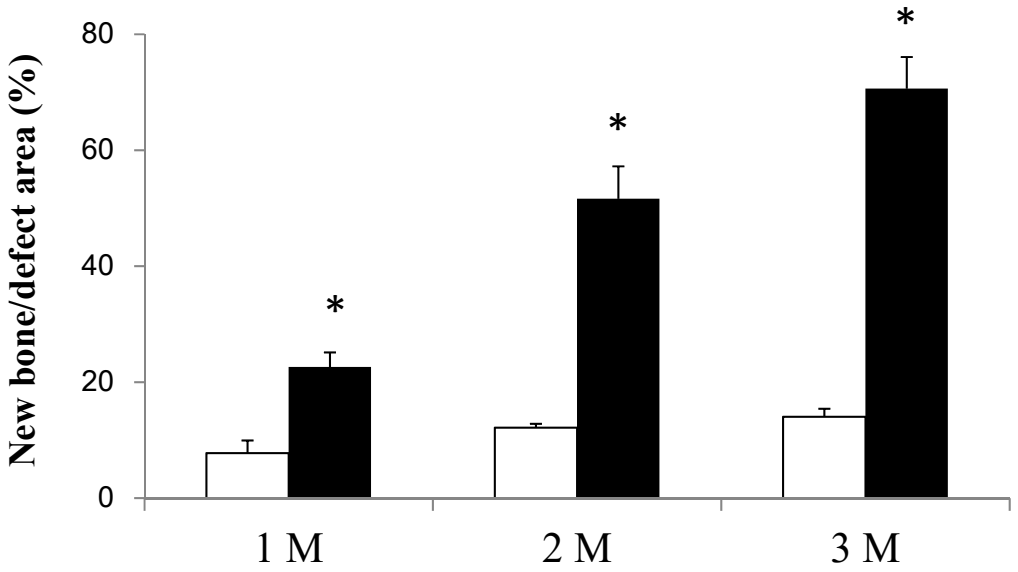


Fig. 3

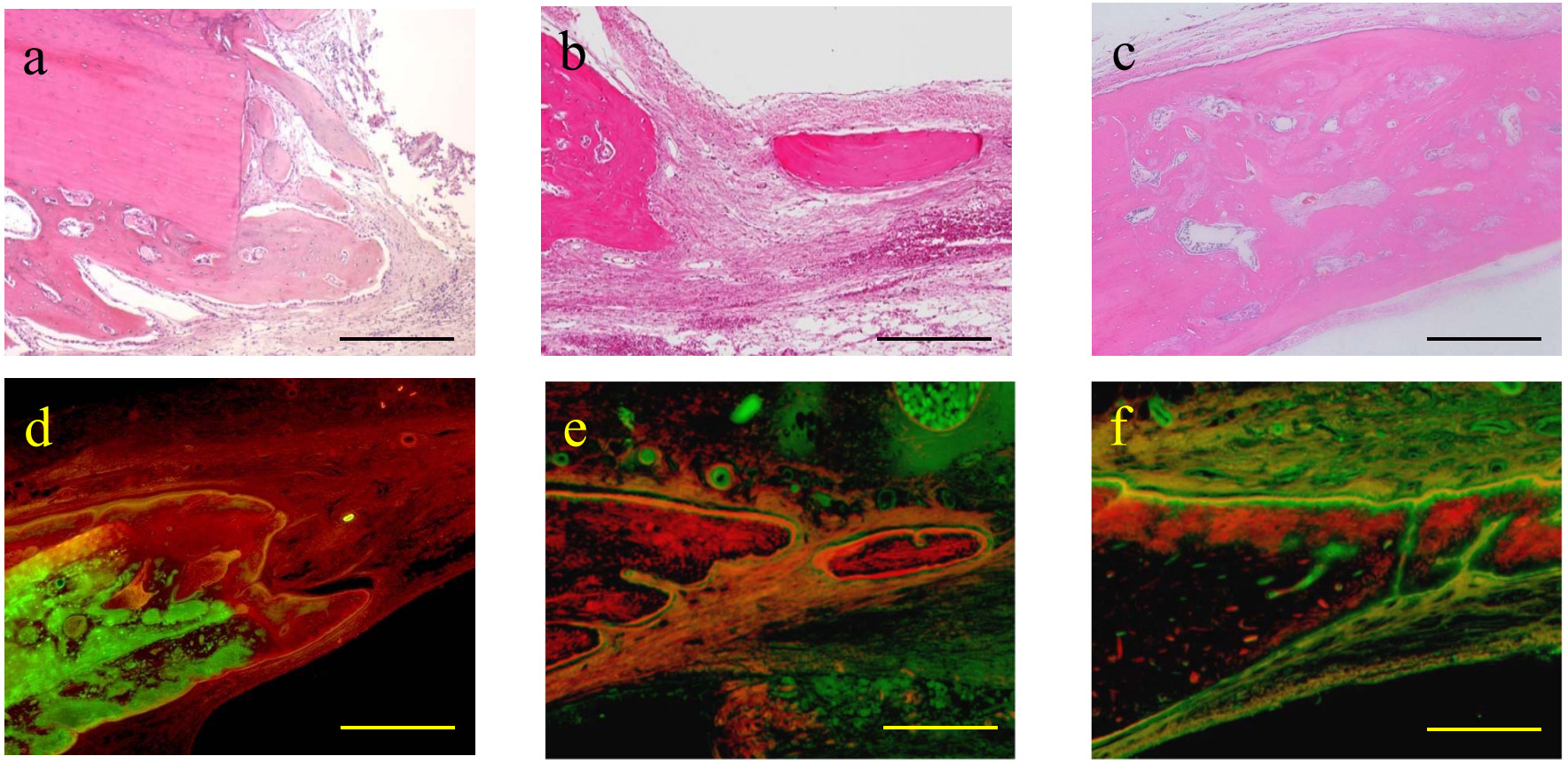


Fig. 4

a

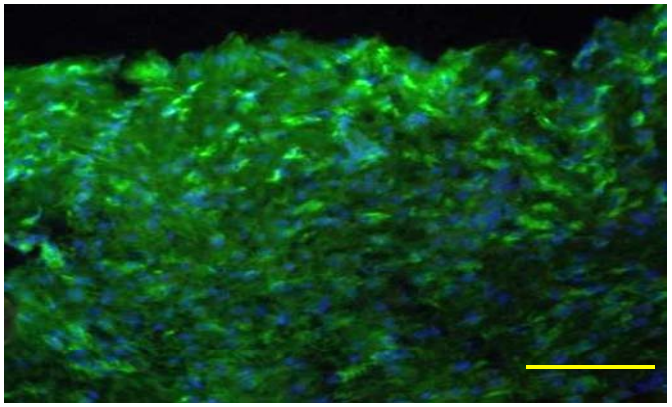

b

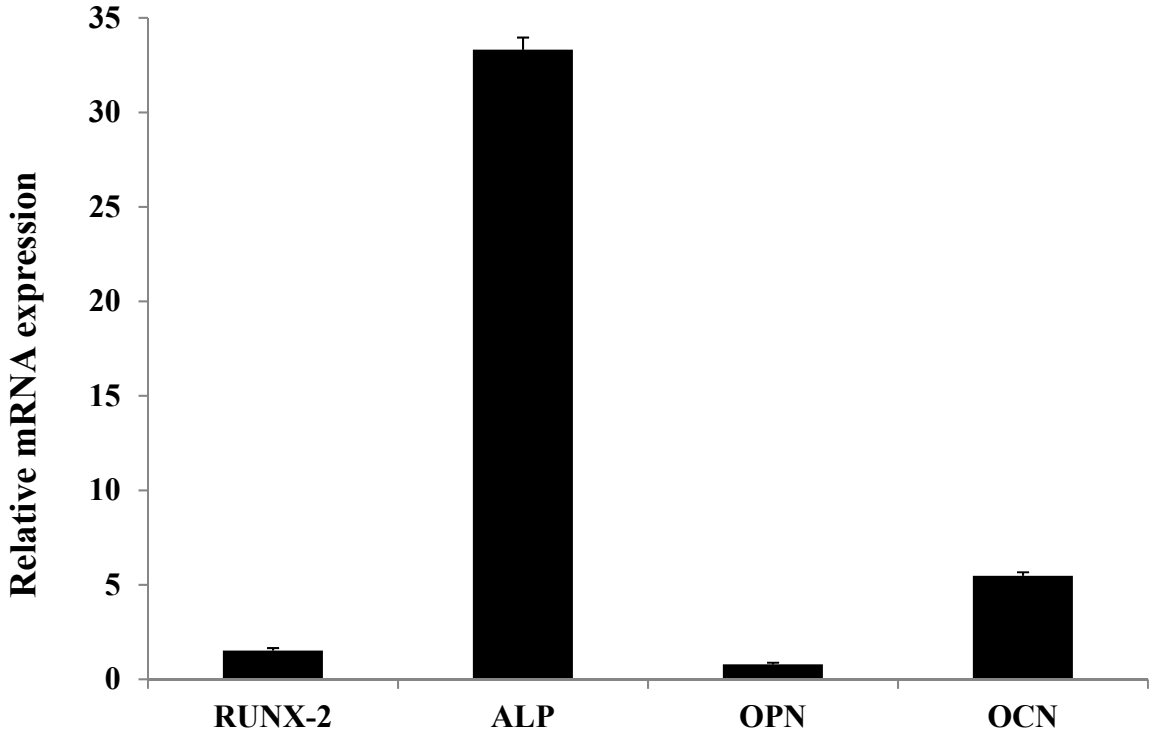
Relative mRNA expression
35
30
25
20
15
10
5
0
RUNX-2
ALP
OPN
OCN

Fig. 5

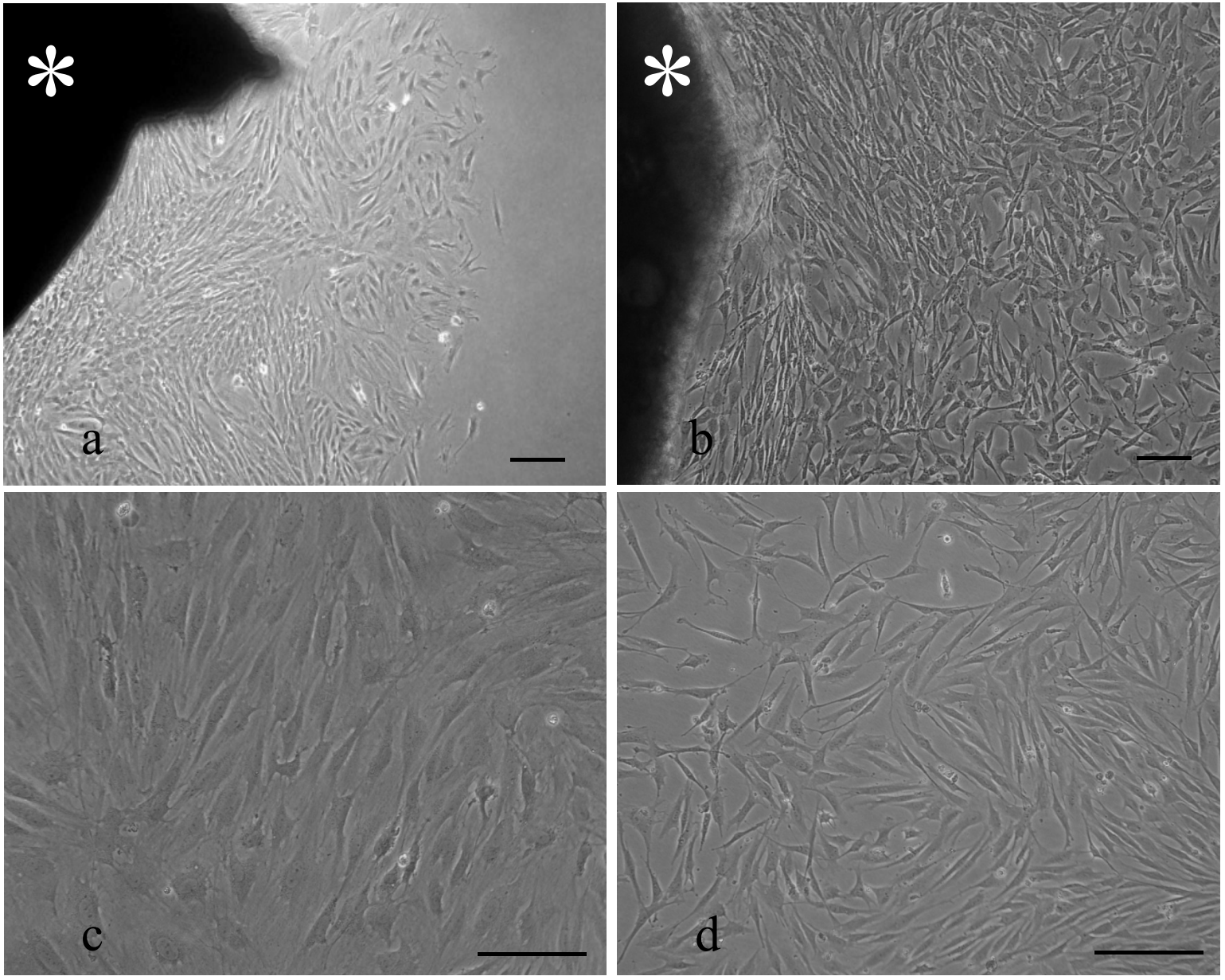


Fig. 6

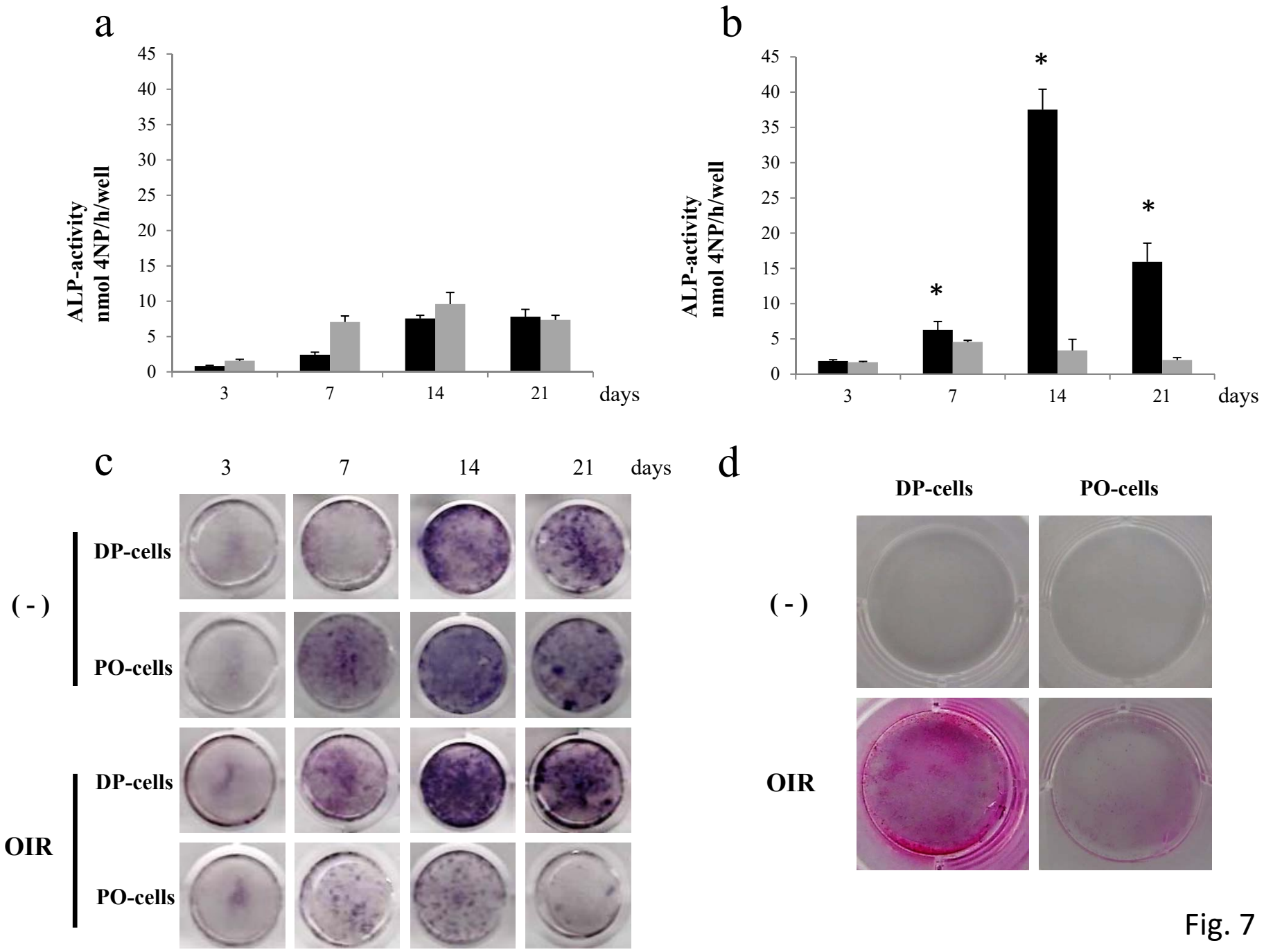
a
ALP-activity
nmol 4NP/h/well
45
40
35
30
25
20
15
10
5
0
3
7
14
21
days
b
ALP-activity
nmol 4NP/h/well
*
*
*
c
3
7
14
21
days
( - )
DP-cells
PO-cells
OIR
DP-cells
PO-cells
d
DP-cells
PO-cells
( - )
OIR

Fig. 7

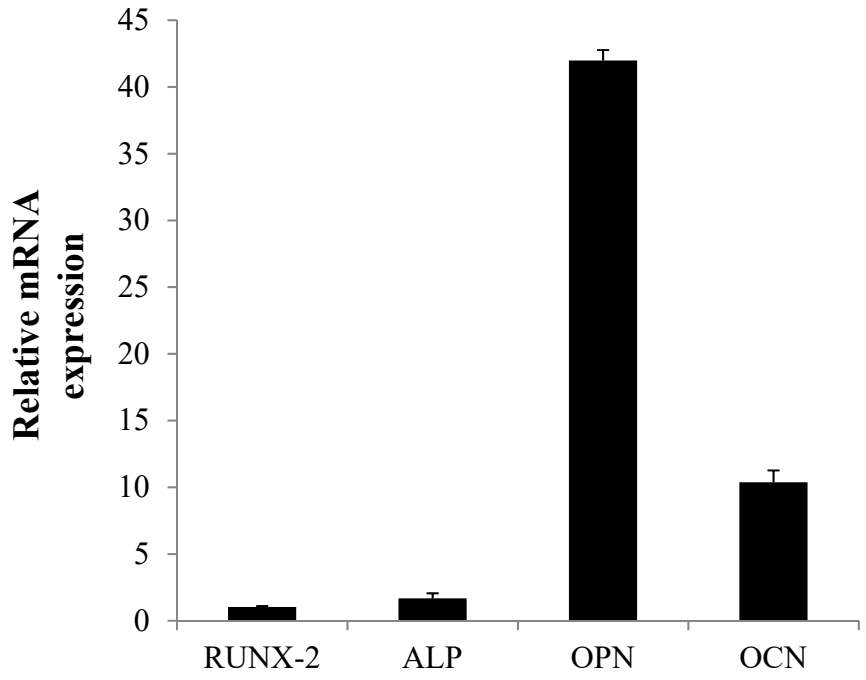
Relative mRNA expression
45
40
35
30
25
20
15
10
5
0
RUNX-2
ALP
OPN
OCN

Fig. 8

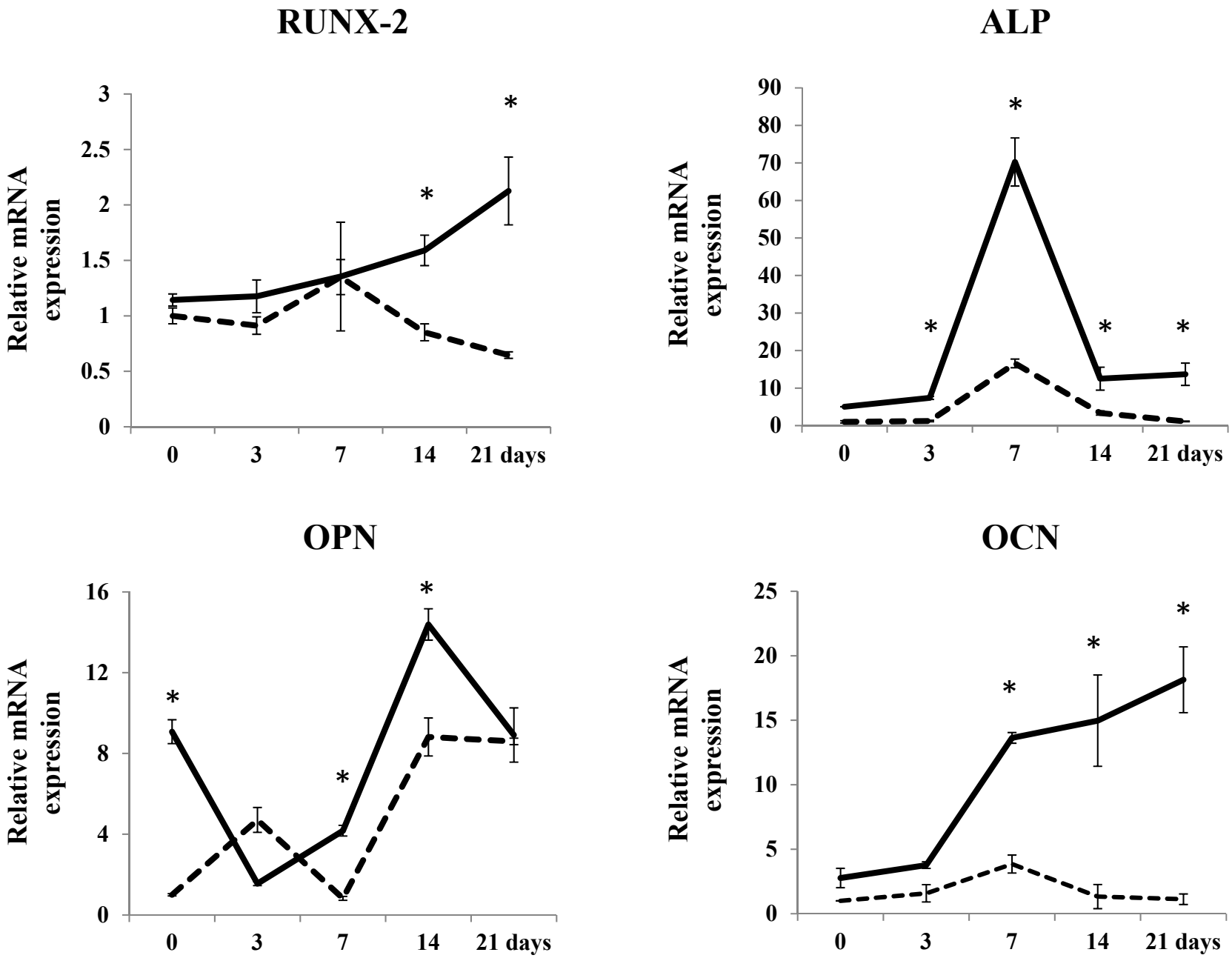
RUNX-2
Relative mRNA expression
3
2.5
2
1.5
1
0.5
0
0
3
7
14
21 days
*
*
*
ALP
Relative mRNA expression
90
80
70
60
50
40
30
20
10
0
0
3
7
14
21 days
*
*
*
*
OPN
Relative mRNA expression
16
12
8
4
0
0
3
7
14
21 days
*
*
*
OCN
Relative mRNA expression
25
20
15
10
5
0
0
3
7
14
21 days
*
*
*

Fig. 9

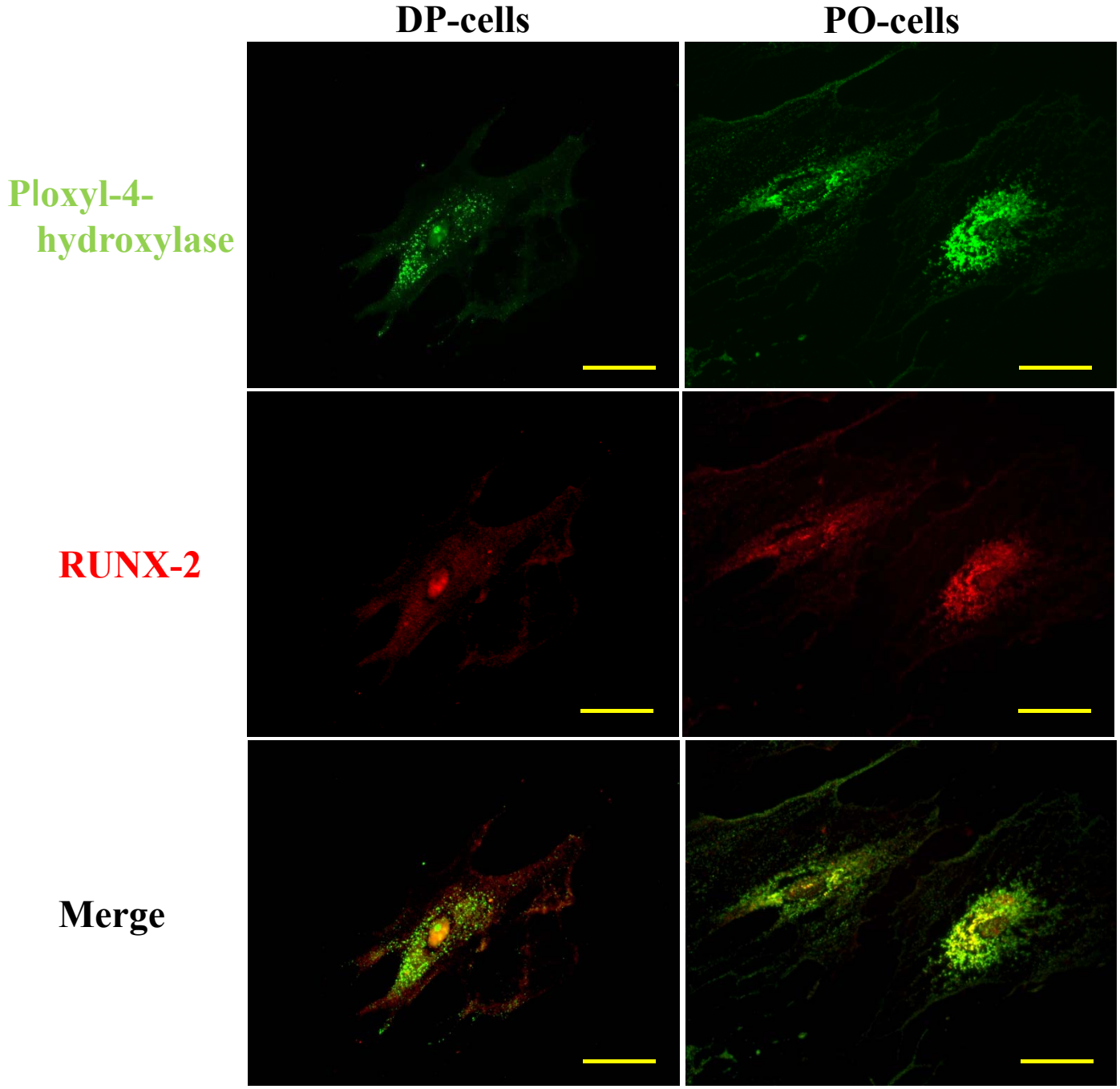


Fig. 10